



## Efficient degradation of nitrobenzene by an integrated heterogeneous catalytic ozonation and membrane separation system with active MgO(111) catalyst

Jun Chen<sup>a</sup>, Shuanghong Tian<sup>a,b,\*</sup>, Lingjun Kong<sup>a</sup>, Yuting Tu<sup>a</sup>, Jiang Lu<sup>a</sup>, Ya Xiong<sup>a,b,\*</sup>

<sup>a</sup>School of Environmental Science & Engineering, Sun Yat-sen University, Guangzhou 510275, P. R. China, Tel. +86 20 84115556; Fax: +86 20 39332690; emails: [chenjunsmile@qq.com](mailto:chenjunsmile@qq.com) (J. Chen), [t-sh-h@163.com](mailto:t-sh-h@163.com) (S. Tian), [kongl\\_jun@163.com](mailto:kongl_jun@163.com) (L. Kong), [524551659@qq.com](mailto:524551659@qq.com) (Y. Tu), [2573801993@qq.com](mailto:2573801993@qq.com) (J. Lu), [cesxya@mail.sysu.edu.cn](mailto:cesxya@mail.sysu.edu.cn) (Y. Xiong)

<sup>b</sup>Guangdong Provincial Key Laboratory of Environmental Pollution Control and Remediation Technology, Guangzhou 510275, P. R. China

Received 18 February 2014; Accepted 21 August 2014

### ABSTRACT

An integrated heterogeneous catalytic ozonation and membrane separation system was studied for continuous degradation of refractory organic pollutants in water. MgO nano-sheets with dominant (111) facets showed large amounts of medium and strong basic sites due to the particular structure of alternating monolayers of exclusively oxygen and exclusively magnesium atoms. MgO(111) acted as the ozonation catalyst for the first time, it was found that efficient degradation of nitrobenzene was achieved with 25.0 mmol/L of MgO (111) catalysts in a wide pH range of 4.0–12.0. In view of practical application, engineering problems to recover fine size catalysts from the treated water were resolved by applying membrane separation technology in the system. Experimental results showed that the membrane could successfully intercept MgO(111) particles in the reactor by the synergistic cooperative sieving of the bare and dynamic membranes. The long-term continuous experiments demonstrated that the removal rate of nitrobenzene could maintain over 90% with a constant flux of 3.92 L m<sup>-2</sup> min<sup>-1</sup> during the 24 h operation. The continuous system provides a new method for practical application of heterogeneous catalytic ozonation to remove refractory organic pollutants.

*Keywords:* Heterogeneous catalytic ozonation; MgO; Membrane separation

### 1. Introduction

Heterogeneous catalytic ozonation, as one of the most promising advanced oxidation processes, has attracted much attention due to its high effectiveness in the degradation and mineralization of refractory organic pollutants and its low negative effect on water quality. It overcomes the limitations of ozone (O<sub>3</sub>) alone process, such as low reaction rate with many

organic compounds, incomplete mineralization, and formation of byproducts [1,2].

Metal oxides (e.g. MnO<sub>2</sub> and TiO<sub>2</sub>) [3,4], supported metal oxides (e.g. MnO<sub>x</sub>/ZrO<sub>2</sub> and FeOOH/Al<sub>2</sub>O<sub>3</sub>) [5,6], and some porous materials (e.g. active carbon and zeolite) [7,8] have been proposed as catalysts for ozonation. These solid catalysts are usually employed in the form of micro- and even nanosize particles in suspension slurries to achieve greater activity since suspend catalysts offer larger active surface area and

\*Corresponding authors.

allow much better contact between the catalysts and pollutants than the immobilized catalysts [6]. Up to now, it has still been a challenge to develop an efficient and stable heterogeneous catalyst for ozonation process. Recently, we prepared MgO nanosheets with dominant (111) facets by facile wet chemical process, which is composed of alternating monolayers of exclusively oxygen and exclusively magnesium atoms [9]. The MgO(111) nanosheets were used as an ozonation catalyst and exhibited high catalytic activity. Moreover, MgO is a simple and nontoxic metal oxide, which is suitable for applications in water treatment.

However, the major concern for the practical application of MgO(111) nanosheets is the separation from the treated water as many other micro- and nanosized catalysts encountered the difficult and time-wasting recovery problem. To resolve the recovery problem, membrane technology appears to be more practical and promising in the heterogeneous catalytic ozonation like in the membrane bioreactors [10,11]. The unit is referred to as a heterogeneous catalytic ozonation and membrane (HCOM) separation reactor in this paper. The membrane acted as a simple barrier for MgO(111) particles and could retain them in the HCOM reactor for immediately continuous reuse. It may obtain some advantages compared to the conventional reactor such as continuous operation of heterogeneous catalytic ozonation process and easy residence time, controlling for pollutant and catalyst. So far, literatures containing both “ozonation” and “membrane” were mainly focused on three aspects: (i) sole ozonation is used as a pretreatment to reduce membrane fouling in the submerged membrane bioreactor process [12,13]; (ii) membrane is used to filter off organic compounds and sole ozonation is used to decrease membrane fouling in a hybrid ozonation-membrane filtration [14–17]; (iii) hollow fiber membrane or porous membrane is used as bubbleless membrane to feed  $O_3$  in order to enhance  $O_3$  mass transfer performance in ozonation process [18,19]. Although many literatures involved both ozonation and membrane filtration technology, none of them mentioned the role of membrane used to separate the fine size catalysts from the treated water. Obviously, the HCOM process has not received attention even though it is expected to possess a technical superiority.

The purpose of this study is to assess the feasibility of an integrated HCOM separation system to remove refractory organic pollutants in water. As part of this project, MgO nanosheets with dominant (111) facets were prepared by facile wet chemical process, and the catalytic activity of MgO(111) in the ozonation of refractory organic pollutants was investigated in a semi-continuous reactor with a view to practical application. The basic characteristics of the HCOM

reactor, including the retention performance of MgO (111) particles, the membrane fouling, and the degradation of organic pollutants, were investigated. Nitrobenzene (NB) was chosen as a model refractory organic pollutant since it is highly toxic, widely dispersed in water and soil, as well as resists oxidation by conventional chemical oxidation and shows poor biodegradability [20].

## 2. Materials and experiments

### 2.1. Materials

The magnesium (Mg) ribbon, methyl alcohol ( $CH_3OH$ ), sodium hydroxide (NaOH), hydrochloric acid (HCl), potassium iodide (KI), sodium thiosulfate pentahydrate ( $Na_2S_2O_3$ ), acetone ( $C_3H_6O$ ), magnesium nitrate ( $Mg(NO_3)_2 \cdot 6H_2O$ ), manganese nitrate ( $Mn(NO_3)_2 \cdot 4H_2O$ ), and tert butyl alcohol ( $C_4H_9OH$ ) were obtained from Tianjin Damao chemical agent factory, China. 4-methoxybenzyl alcohol ( $C_8H_{10}O_2$ ) was got from Aladdin chemistry Co. Ltd, China. Nitrobenzene ( $C_6H_5NO_2$ ) was purchased from Guangzhou chemical reagent Co. Ltd, China. All chemicals were analytical grade and used without further purification. The ceramic micro-filtration membrane module (MT-3) was provided by Midea Co. Ltd, China. The membrane is a hollow cylinder which has an outer diameter of 50 mm, an inner diameter of 48 mm, a length of 70 mm, with an average pore size of  $3.0 \mu m$ , and the surface area of  $0.0085 m^2$ . Pure water was used to prepare solutions.

### 2.2. Preparation of catalyst

The catalyst of MgO with dominant (111) facets was prepared by reported wet chemical process [9]. Briefly, the Mg ribbon (1.67 g) washed with  $C_3H_6O$  was reacted with absolute  $CH_3OH$  (70 mL) in a flask to obtain the inorganic intermediate magnesium methoxide. Then  $C_8H_{10}O_2$  (4.35 mL) was added to the above flask. After stirred for 5 h, the mixture solvent of 2.50 mL of pure water and 50 mL of absolute  $CH_3OH$  was added dropwise and stirred for 12 h. Subsequently, the mixture was transferred to a 1 L high pressure reactor under the argon atmosphere for supercritical treatment. The obtained white powder was calcined at  $500^\circ C$  for 6 h with heating rate of  $3^\circ C/min$ , producing the final catalyst of MgO.

### 2.3. Construction of HCOM reactor and catalytic activity measurements

The integrated reactor of HCOM separation, namely a HCOM reactor, was constructed as shown in

Fig. 1. The HCOM reactor consists of a reaction cylinder, catalyst particles, a submerged ceramic membrane module, an O<sub>3</sub> feed system, a wastewater feed system, an effluent collecting system, and O<sub>3</sub> traps. The reaction cylinder with several input/output ports has a height of 615 mm, and an inner diameter of 65 mm. The O<sub>3</sub> feed system includes an O<sub>3</sub> generator (YE-TG-II, Nanjing YDG ozone Co., Ltd, China) and an online O<sub>3</sub> detector (IDEAL-2000, IDEAL USA). In a typical experimental run, 900 mL pure water was added into the reaction cylinder. O<sub>3</sub> gas was produced from cylinder oxygen by the O<sub>3</sub> generator and diffused into the reactor through a corundum sparger at a flow rate of 0.5 L/min monitored by a flow meter on the generator. The O<sub>3</sub> gas concentration in the stream containing O<sub>3</sub> and oxygen was controlled at  $5.0 \pm 0.2$  mg/L monitored by the O<sub>3</sub> detector. The excess O<sub>3</sub> in the outlet gas was trapped by KI solution. After reaching the steady-state condition in 20 min, 100 mL of NB solution (500.0 mg/L) and a certain amount of catalyst were added into the reaction cylinder. At the same time, NB aqueous solution (50.0 mg/L) was supplied into the reactor continuously by one pump at a flow rate of 33.3 mL/min. The treated water permeated through the membrane driven by another pump at the same flow rate of 33.3 mL/min in order to keep the solution volume constant in the reactor cylinder. With this flow rate, the hydraulic retention time was controlled to be

30 min. Thus, MgO particles can be retained in the reactor by the membrane module. The O<sub>3</sub> gas concentration, system pressure, and flux were monitored and recorded on an online computer throughout the operation of the HCOM reactor. At a given time interval, 5 mL of sample was taken by the sampling valve set at the upper reaction cylinder to quantify adsorption/oxidation. 0.05 mL of 0.25 mol/L Na<sub>2</sub>S<sub>2</sub>O<sub>3</sub> was subsequently added to quench the aqueous O<sub>3</sub> remaining in the reaction solution. Then samples were analyzed immediately after filtration through 0.22 μm Millipore membrane filters. The reaction temperature was maintained at 25°C.

The catalytic activity of MgO(111) nanosheets in the heterogeneous catalytic ozonation process was evaluated by comparing with the conventionally prepared MgO (CP-MgO), varying catalyst dosage, the initial solution pH value, and the amount of radical scavenger tert butyl alcohol (TBA) in a semi-continuous reactor. All the semi-continuous experiments were also carried out in the above reactor except that total 1 L of NB solution was added into the reactor and no influent and effluent were supplied.

#### 2.4. Characterization of catalysts and analytical methods

The TEM measurements were carried out on a FEI Tecnai G2 Spirit (FEI, Netherlands) operated at 120 kV or 300 kV. The specific surface area and temperature programmed desorption of carbon dioxide (CO<sub>2</sub>-TPD) were determined with an Autosorb-iQ-MP gas sorption analyzer (Quantachrome Instruments, USA) [21]. The XRD pattern was obtained by using D/max 2200 vpc Diffractometer (Rigaku Corporation, Japan) with a Cu Kα radiation at 30 kV and 30 mA. The particle size and zeta potential were measured by particle size and zeta analyzer (Zetasizer Nano-ZS 90, Malvern), respectively. The turbidity was determined using a turbidimeter (Model 2100 N, Hach). The pH of the solution was measured with a PHS-3C pH meter (Rex instrument factory, Shanghai, China). The concentration of NB was analyzed by means of a high performance liquid chromatography (HPLC, LC15, Shimadzu, Japan) with a UV detector (SPD-15C) at 262 nm. A Wondasil 5 μm C18 column (4.6 × 150 mm, GL Sciences, Inc) was used and kept at 30°C. The mobile phase was a mixture of methanol and water at 70:30 (v/v), and its flow rate was 1.0 mL/min. The total organic carbon (TOC) of the reaction mixture was measured on a TOC analyzer (Shimadzu, Japan). The gas concentration of O<sub>3</sub> was measured by ultraviolet absorption method through an online O<sub>3</sub> detector (IDEAL, USA). The pressure was measured by

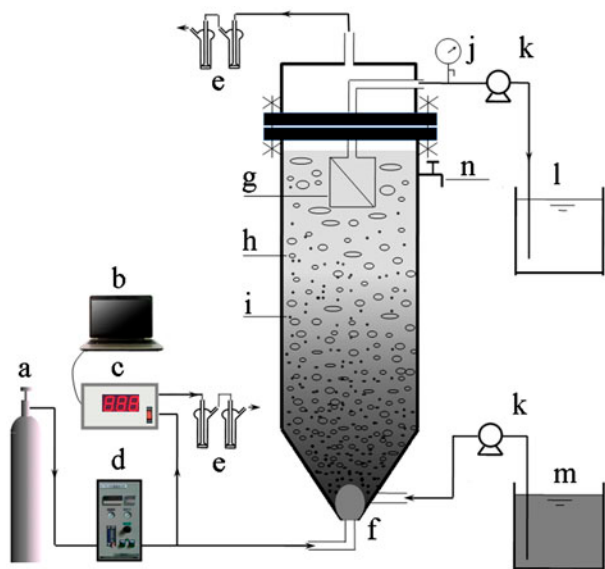


Fig. 1. Schematic diagram of the HCOM reactor: (a) oxygen cylinder, (b) PC monitor, (c) O<sub>3</sub> detector, (d) O<sub>3</sub> generator, (e) KI trap, (f) reaction cylinder, (g) membrane module, (h) bubbles, (i) catalyst particles, (j) manometer, (k) pump, (l) effluent tank, (m) waste water feed tank, (n) sampling port.

micro-manometer (ZhengBao, YE-60, China) and the membrane resistance was measured according to the literature [22]. The concentrations of magnesium ions were detected by an inductively coupled plasma (ICP) atomic emission spectrometer (5300DV, PE, USA).

### 3. Results and discussion

#### 3.1. Characterization of MgO

As shown in Fig. 2(a), the morphology of periclase MgO in TEM image is similar to that reported in the literature [9] and presented as nanosheets with irregular shape. Moreover, most of the nanosheets are oriented parallel to the support film while some of the

sheets are imaged edge on, from which the thickness of the sheet is determined as about 4.80 nm. As shown in Fig. 2(b), HRTEM image and local Fourier transform (FFT) of isolated MgO nanosheets exhibit lattice fringes with a distance of 0.24–0.25 nm parallel to the main surface of the nanosheet is in good agreement with the (111) lattice spacing of MgO, indicating that their main surface of MgO nanosheets is parallel to the (111) lattice planes. As it is well known, the MgO (111) facet is composed of alternating monolayers of exclusively oxygen and exclusively magnesium atoms. In contrast, the conventionally prepared MgO (CP-MgO) by thermal decomposition of either magnesium salts or magnesium hydroxides possess the (100) facets as their primary surface [23]. Compared to

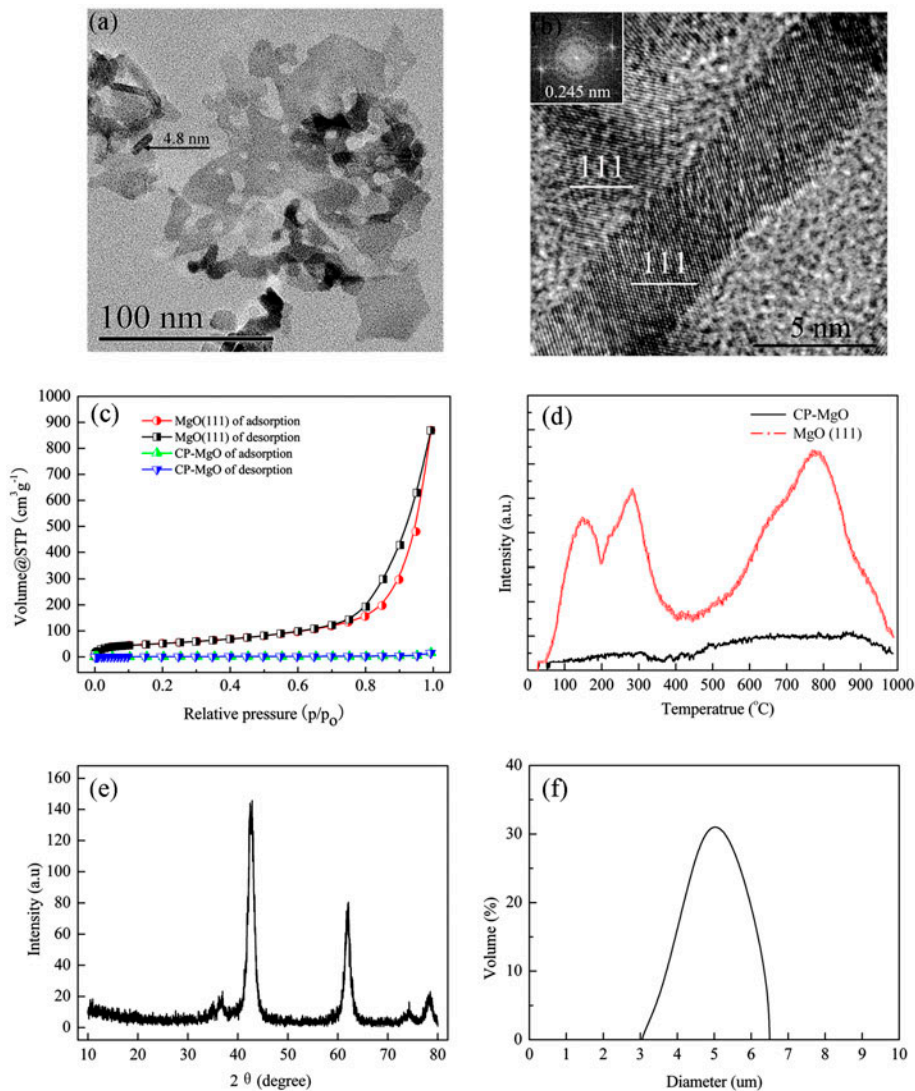


Fig. 2. Characteristics of the prepared MgO powder: (a) TEM image; (b) HRTEM image and local FFT; (c) nitrogen adsorption–desorption isotherms; (d) CO<sub>2</sub>-TPD of MgO(111) and CP-MgO; (e) XRD pattern; (f) particle size distribution.

CP-MgO, the surface of MgO(111) has a strong electropolarity, high surface reactivity, and large amounts of stronger basic sites on the surface due to high concentration of surface  $O^{2-}$  Lewis basic sites corresponding to the particular structure of MgO(111) with pure  $O^{2-}$  on one layer [21]. These characteristics may pose positive effects in heterogeneous catalytic ozonation [24]. In an attempt to prove the strong solid basic characteristics of MgO(111) directly, the  $CO_2$ -TPD measurements on MgO(111) and CP-MgO were carried out for comparisons (Fig. 2(d)). The TPD profile of MgO(111) contains three  $CO_2$  desorption peaks. The first two peaks are partly overlapped, widely ranged from 25 to 400°C. The peaks between 25 and 200°C could be attributed to the interaction of  $CO_2$  with the weak basic sites that correspond to hydroxyl groups on the surface. The second group between 200 and 400°C may be associated with oxygen in the  $Mg^{2+}$  and  $O^{2-}$  pairs. Finally, the peak higher than 400°C may be due to the existence of strong basic sites, possibly corresponding to isolated  $O^{2-}$  [25]. Generally speaking, the strength of basic sites increases with the increasing temperature of the peaks appeared in the TPD profile, and the larger peak area corresponds to more basic sites. It is obvious that MgO(111) nanosheets obtained more basic sites indicating the large peak areas in the whole temperature range. Particularly, there are much more medium and strong basic sites on the surface of MgO(111) nanosheets than CP-MgO nanocrystals directly derived from the calcination of  $Mg(NO_3)_2$ . The nitrogen adsorption–desorption isotherms of the samples are shown in Fig. 2(c). The synthesized MgO(111) and CP-MgO have the specific surface area of 187.8 and 13.4  $m^2/g$ , calculated from the linear region of the Brunauer–Emmett–Teller (BET) plot. The average pore volume and size are 1.38  $cm^3/g$  and 12.45 nm for MgO(111), while 0.023  $cm^3/g$  and 6.87 nm for CP-MgO, calculated from the nitrogen desorption isotherm by the Barrett–Joyner–Halenda method. Obviously, MgO(111) has higher BET than CP-MgO. The XRD pattern of the fabricated MgO powder in Fig. 2(e) confirms the pure periclase MgO crystalline (JCPDS file No. 45-0946). As shown in Fig. 2(f), the prepared MgO particles suspended in aqueous solution possesses particle size distribution from 3.09 to 6.44  $\mu m$  with an average particle size of 4.67  $\mu m$ . Thus, a micro-filtration membrane with high permeate flux can be selected to intercept MgO(111) nanosheets in the reactor.

Zeta potentials of MgO(111) nanosheets were measured at various pH values to examine the surface charge and basic properties. As shown in Fig. 3, the  $pH_{PZC}$  (pH at which the surface has the point of zero charge) of MgO(111) is located at pH 12.7, which is

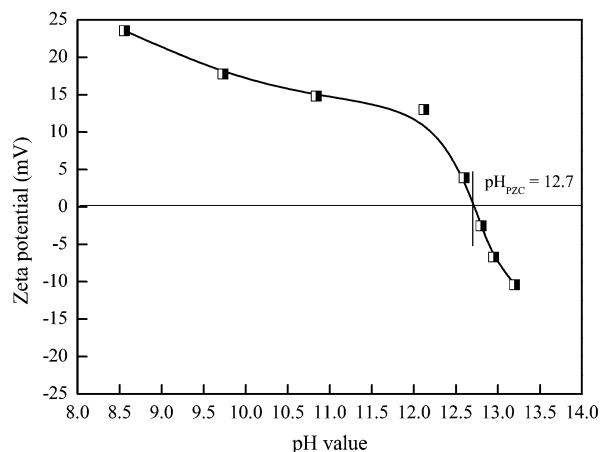


Fig. 3. Zeta potential at various pH values of the prepared MgO.

higher than that of 12.4 [26]. It is well known that the  $pH_{PZC}$  values of the oxides are in accordance with their acid/base properties, higher  $pH_{PZC}$  corresponds to higher basic character [27,28]. Hence, the high  $pH_{PZC}$  of MgO(111) suggests that MgO(111) possesses strong basic property, in accordance with the result of  $CO_2$ -TPD measurement. Below pH 12.7, the surface of MgO(111) is positively charged and counterbalanced ions  $OH^-$  are attracted, thus the basic micro-environment near the surface of MgO(111) particles forms, which facilitates the generation of hydroxyl radicals ( $\cdot OH$ ) from  $O_3$ .

### 3.2. Batchwise catalytic degradation of NB

In an attempt to evaluate the catalytic degradation of NB in suspension system, a series of comparison experiments were done by varying catalyst types and dosage, the initial solution pH value, and the amount of radical scavenger TBA. The investigations can also supply a theoretic optimal reaction condition in the HCOM reactor operated in continuous flow mode.

#### 3.2.1. Effect of catalyst types and dosage

Effect of catalyst types were investigated on the degradation of NB. As shown in Fig. 4(a), the degradation efficiencies of NB were 90.6 and 70.2% in MgO(111)/ $O_3$ , CP-MgO/ $O_3$  within 30 min reaction when fixing the catalyst dosage at 25.0 mmol/L. It is obvious that MgO(111) promoted the degradation of NB much more significantly than CP-MgO. This indicated that the prepared MgO(111) displayed higher catalytic activity in ozonation than CP-MgO. Compared to

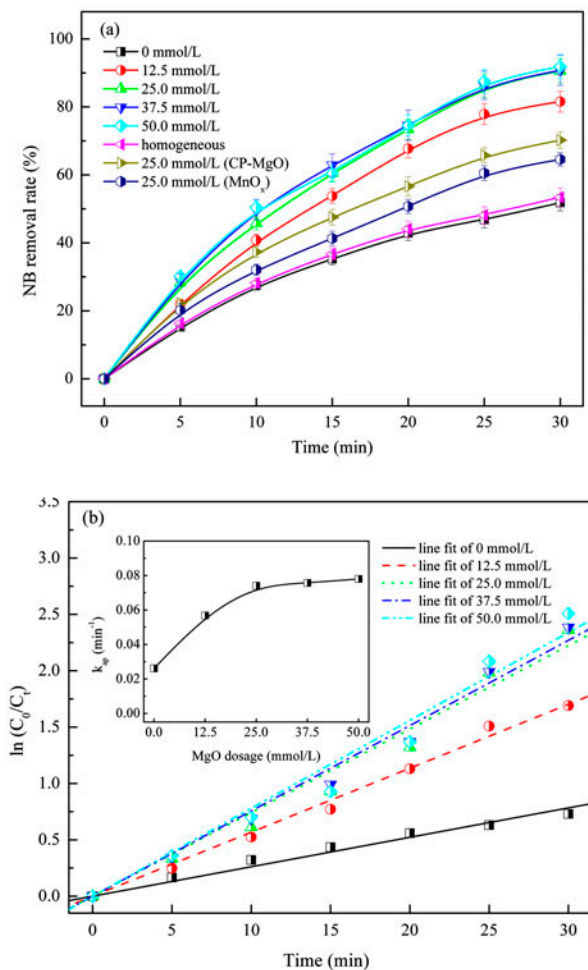


Fig. 4. (a) Effect of catalyst types and MgO(111) dosages on NB degradation. CP-MgO and MnO<sub>x</sub> derived from the thermal decomposition of magnesium nitrate and manganese nitrate (O<sub>3</sub>: 5.0 mg/L; NB: 50.0 mg/L; pH: 6.7); (b) Line fit of kinetics data with different catalyst dosages of MgO(111), insert: the  $k_{ap}$  at different MgO(111) dosages.

CP-MgO, the surface of MgO(111) has larger amounts of medium and strong basic sites on the surface due to a high concentration of surface O<sup>2-</sup> Lewis basic sites corresponding to the particular structure of MgO (111) with pure O<sup>2-</sup> on one layer, which has been proved by CO<sub>2</sub>-TPD measurements in Fig. 2(d). Moreover, the surface of solid base MgO(111) is positively charged and counterbalanced ions OH<sup>-</sup> are attracted, thus the basic micro-environment near the surface of MgO(111) particles forms below pH 12.7. Both the presence of large amounts of basic sites and the basic micro-environment facilitates the generation of ·OH from O<sub>3</sub> [29]. Thus, organic pollutants can be oxidized efficiently in MgO(111)/O<sub>3</sub> system. Manganese oxide (MnO<sub>x</sub>) is the most extensively studied catalyst in the ozonation. Zhao et al. reported that the home-made

MnO<sub>x</sub> can remove aqueous NB efficiently under their investigated conditions [30]. Herein, MnO<sub>x</sub> prepared according to Zhao's method was also used as ozonation catalyst for comparisons. The results showed that the presence of MnO<sub>x</sub> enhanced the degradation of NB in the ozonation, but the enhancement degree was lower than both MgO(111) and CP-MgO. The results showed that MgO(111) exhibited the highest catalytic activity towards the degradation of NB in ozonation. Hence, MgO(111) was selected as the catalyst in all the following experiments.

A sufficient amount of catalyst is needed to ensure enough catalytic active sites and thus maintain efficient catalytic ozonation in the reactor. However, higher catalyst dosage has some negative effects, such as lower critical flux, more serious membrane fouling as well as higher operational cost. The effect of the MgO catalyst dosage on the degradation of NB was further investigated, as shown in Fig. 4(a). Usually, the removal of organic pollutant by O<sub>3</sub> is first order with respect to O<sub>3</sub> and the pollutant. When the amount of O<sub>3</sub> is in excess, the reaction is pseudo-first-order with respect to organic pollutant [31]. A pseudo-first-order linear relationship was observed in the plot of  $\ln(C_0/C_t)$  vs. reaction time, as shown in Fig. 4(b). The apparent rate constant of NB degradation in the ozonation alone process or in the catalytic ozonation process can be calculated according to the equation of  $\ln(C_0/C_t) = k_{ap} t$ , where  $k_{ap}$  is the slope of the curve in Fig. 4(b). The lowest degradation efficiency of NB appeared in the absence of MgO, namely in the ozonation alone process, with the removal rate of only 51.8% and the  $k_{ap}$  value of 0.0261 min<sup>-1</sup> within 30 min reaction. When 25.0 mmol/L of MgO(111) was added to the reaction system, both the removal rate of NB and the  $k_{ap}$  value increased to 90.6% and 0.0741 min<sup>-1</sup>, respectively, within 30 min reaction. After that, further increasing MgO(111) catalyst dosage to 37.5 mmol/L and even 50.0 mmol/L, the  $k_{ap}$  value showed relative steady, indicating that catalyst dosage of more than 25.0 mmol/L would not accelerate the catalytic ozonation. It was because a small amount of MgO(111) made it possible that the chain of radical reactions could be induced and propagated by the O<sub>3</sub> introduced in the reactor, while the excess catalyst easily aggregated and affected the usage efficiency [32]. Thus, 25.0 mmol/L of MgO(111) was selected as the optimum dosage for the following experiments. To make it certain how much homogeneous catalytic ozonation originated from the leached magnesium contributed to the degradation of NB. The homogeneous filtrate of the 25.0 mmol/L MgO(111) slurry after being aerated with air for 30 min was collected. The homogeneous catalytic ozonation was

conducted by adding the concentrated NB and inletting  $O_3$  to the filtrate. The initial NB concentration was also controlled at 50.0 mg/L. The results suggested that the degradation curve of the homogeneous catalytic ozonation almost overlapped that of the ozonation alone in Fig. 4(a). Hence, it was deduced that the degradation of NB in MgO(111)/ $O_3$  system is mainly contributed by the heterogeneous catalytic ozonation, not the homogeneous catalytic ozonation.

### 3.2.2. Effect of the initial solution pH value

In the catalytic ozonation process, solution pH value can affect the decomposition rate of the dissolved  $O_3$ , the surface properties of catalyst, and the dissociation of ionic or ionizable organic molecules, which would finally determine the degradation of pollutants [33]. Therefore, effect of the initial solution pH value on NB degradation in MgO(111)/ $O_3$  system was studied (Fig. 5). As can be seen from Fig. 5(a), increasing the initial pH from 4.0 to 6.7 led to an enhancement of NB removal rate from 80.9 to 90.6% at 30 min, which increased to 92.8% when further increasing the initial pH value to 8.0, and even to slightly higher value with the pH adjusted to 10.0 and 12.0. It could be observed that the degradation efficiency of NB catalyzed by MgO(111) was located between 80.9 and 95.7% in a wide pH range of 4.0–12.0 within 30 min. It means no pH adjustment to the wastewater, as pretreatment, is needed for MgO(111)/ $O_3$  process in a wide pH range. This observation is very important for the practical industrial application of catalytic ozonation in wastewater treatment. Zhao et al. [34] also found higher NB removal rate at a higher pH value in the catalytic ozonation of NB by ceramic honeycomb. As it is well known, water pH indicates the concentration of  $OH^-$  in the solution, which is an initiator for aqueous  $O_3$  decomposition into  $\cdot OH$  [35]. When pH increased, especially in alkaline pH value, more  $OH^-$  could initiate  $O_3$  decomposition to form  $\cdot OH$ , which had high reaction activity towards NB. Especially, when the initial solution pH increased over 12.0, the surface of MgO(111) was negatively charged and  $MgO-O^-$  was the dominant species since the  $pH_{PZC}$  of MgO(111) is 12.7. The negatively charged surface favors the interaction of  $O_3$  with the catalyst. This is an important property for enhancement of transformation of  $O_3$  into  $\cdot OH$ . Even some studies indicate that the deprotonated surface groups of the catalyst can act as initiators of radical reactions [36]. These reasons resulted in high removal rate of NB at high pH conditions. In contrast, less  $OH^-$  in the solution was obtained at acidic conditions. However, MgO(111) possesses alkaline property and

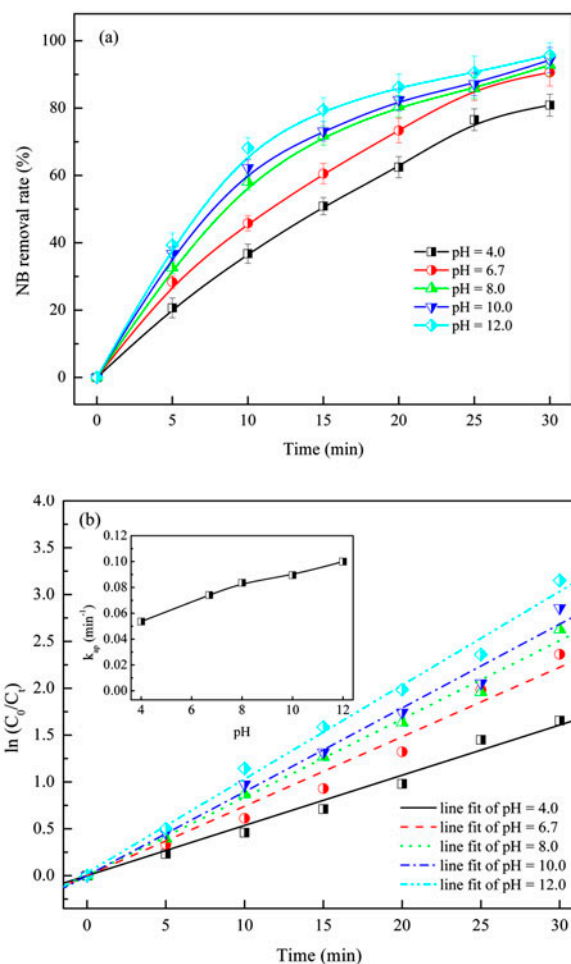


Fig. 5. (a) Effect of the initial solution pH value on NB degradation (MgO: 25.0 mmol/L;  $O_3$ : 5.0 mg/L; NB: 50.0 mg/L); (b) Line fit of kinetics data with different initial solution pH value, insert: the  $k_{ap}$  of different initial solution pH value.

the  $pH_{PZC}$  is 12.7. Below pH 12.7, the surface of MgO(111) is positively charged and counterbalanced ions  $OH^-$  are attracted, thus the alkaline micro-environment near the surface of MgO(111) particles forms, which facilitates the generation of  $\cdot OH$ . This result accords with the report that reactive oxygen species such as  $\cdot OH$ , superoxide radicals, and hydrogen peroxide formed on the surface of MgO which is covered by a layer of  $OH^-$  in the field of antibacterium [37]. The formation of the alkaline micro-environment may explain high removal rate of NB at low pH conditions. Although high NB conversion at 30 min was achieved in a wide pH range of 4.0–12.0 and no remarkable difference in the removal rate of NB at 30 min was observed at different initial pH value, the rate constant  $k_{ap}$  of NB degradation increased from 0.0536 min<sup>-1</sup> at

pH 4.0 to  $0.0741 \text{ min}^{-1}$  at pH 6.7 as shown in Fig. 5(b). When the pH is increased to 12.0, the  $k_{\text{ap}}$  value is further increased to  $0.1000 \text{ min}^{-1}$ . The results revealed that increasing the initial pH value can promote the NB degradation and MgO(111) is the highly active catalyst in the ozonation in a wide pH range.

### 3.2.3. Effect of the addition of radical scavenger TBA

TBA is a strong radical scavenger to terminate the radical chain reaction, which has the reaction rate constant of  $6 \times 10^8 \text{ M}^{-1} \text{ s}^{-1}$  with  $\cdot\text{OH}$  and only  $3 \times 10^{-3} \text{ M}^{-1} \text{ s}^{-1}$  with  $\text{O}_3$  [38]. It is generally believed that  $\text{O}_3$  reacts with various organic pollutants in aqueous solution by a direct reaction of  $\text{O}_3$  or through a radical type reaction involving  $\cdot\text{OH}$  induced by  $\text{O}_3$  decomposition in water. To make it clear whether  $\cdot\text{OH}$  are involved in the ozonation alone process and the catalytic ozonation process, TBA (100.0 mg/L) was added to the initial solution. As shown in Fig. 6(a), after the addition of TBA, the NB removal rate decreased from 90.6 to 62.8% in MgO(111)/ $\text{O}_3$  process. It was obvious that the  $\cdot\text{OH}$ , able to oxidize NB more efficiently, were quenched by TBA. This indicated that the degradation mechanism of NB in MgO(111)/ $\text{O}_3$  involved  $\cdot\text{OH}$  reaction mechanism. In the same situation,  $\cdot\text{OH}$  was also involved in ozonation alone indicated by the decrease in the NB removal rate from 51.8 to 40.3%, which is consistent with Ren's result [39]. Furthermore, the percentages of  $\text{O}_3$  and  $\cdot\text{OH}$  contribution to total oxidation were calculated. Since the TBA was added to capture the  $\cdot\text{OH}$ , the removal rates of NB can be attributable to the oxidation by ozonation alone. Considering that the total oxidation were mainly resulted by the oxidation of  $\text{O}_3$  and  $\cdot\text{OH}$ , the contribution by  $\cdot\text{OH}$  ( $f_{\text{OH}}$ ) and  $\text{O}_3$  ( $f_{\text{O}_3}$ ) can be estimated by Eq. (1) [40].

$$f_{\text{OH}} = 1 - f_{\text{O}_3} = \left(1 - \frac{k_{\text{TBA}}}{k_{\text{ap}}}\right) \times 100\% \quad (1)$$

where  $k_{\text{TBA}}$  is the slope of the curve oxidation NB when TBA was added in the reaction processes. The linear regression of the data got from Fig. 6(a), the  $k_{\text{TBA}}$  and  $k_{\text{ap}}$  were 0.0341 and  $0.0741 \text{ min}^{-1}$  within 30 min reaction in MgO(111)/ $\text{O}_3$  process, and 0.0175 and  $0.0261 \text{ min}^{-1}$  in ozonation alone process. Hence, the  $f_{\text{O}_3}$  and  $f_{\text{OH}}$  were 46.0 and 54.0% at 30 min in MgO(111)/ $\text{O}_3$  process while 67.0 and 33.0% in ozonation alone process. Obviously, the  $\cdot\text{OH}$  contribution in the former process had at least 1.6 times as much as that in the latter process. The effect of TBA and mineralization

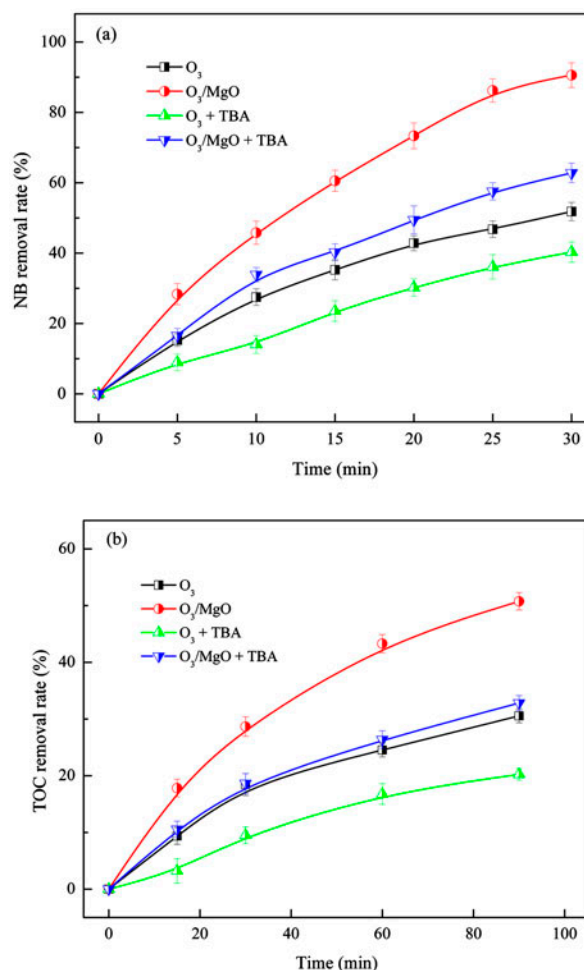


Fig. 6. (a) Effect of TBA on NB degradation in different processes; (b) Effect of TBA on TOC degradation in different processes (TBA [if use]: 100.0 mg/L; MgO: 25.0 mmol/L;  $\text{O}_3$ : 5.0 mg/L; NB: 50.0 mg/L; pH: 6.7).

of NB were evaluated by the TOC removal rate in the MgO(111)/ $\text{O}_3$  process, which was also measured in ozonation alone process for comparisons, as shown in Fig. 6(b). For both processes, the TOC removal rate increased with increasing reaction time. At 90 min, the TOC removal rate in MgO(111)/ $\text{O}_3$  process in the absence of TBA reached 50.8%, 20.0% higher than that of ozonation alone process. This indicated that the presence of MgO(111) exerted very positive influence on the TOC removal rate. When the addition of TBA, the TOC removal rate both decreased to 32.8 and 20.2% in MgO(111)/ $\text{O}_3$ , and ozonation alone process, also indicated the degradation mechanism of NB involved  $\cdot\text{OH}$  reaction mechanism.

### 3.3. Continuous catalytic degradation of NB in HCOM reactor

#### 3.3.1. Retention of catalyst particles by the membrane

Although MgO(111) nanosheets exhibited high catalytic activity towards the degradation of refractory organic pollutants, the difficult and time-wasting recovery of the catalyst decreased the water treatment efficiency greatly. Hence the separation of the suspended catalysts became the major concern for the practical application of MgO(111) nanosheets. Inspired by the idea of MBR, the membrane was introduced into the heterogeneous catalytic ozonation reactor to intercept the catalyst particles similar to MBR technology [10,11] since fine catalyst particles being suspended in the solution is just like the activated sludge particles being suspended in wastewater in activated sludge process. Thus, the recovery problem of fine size catalyst particles was possibly resolved.

According to Cherkasov and Polotsky's report [41], the value of the critical ratio,  $F_{cr} = r_s/R_h$  was 0.7–1.0 for micro-filtration, where  $r_s$  is the minimal radius of particles retained by the membrane and  $R_h$  is the mean hydraulic pore radius. Since the minimal diameter of MgO(111) particle suspended in aqueous solution was  $3.09\ \mu\text{m}$ , a commercial ceramic membrane with an average surface pore size of  $3.0\ \mu\text{m}$  was selected and applied in the continuous-flow HCOM reactor ( $F_{cr} = 1.0$ ).

Retention of MgO(111) catalyst particles by the micro-filtration membrane in the HCOM reactor was evaluated by both turbidity and residual catalyst concentration in the suspended solution under constant trans-membrane pressure (TMP) (Fig. 7). The dosage of MgO(111) catalyst in HCOM reactor was 12.5, 25.0, 37.5, and 50.0 mmol/L, corresponding to the turbidity of 61 NTU, 270 NTU, 400 NTU, and 480 NTU, respectively. In all cases, the turbidity of the mixed liquor inside the HCOM reactor decreased at the beginning and then reached a steady-state value of 47 NTU, 235 NTU, 281 NTU, and 378 NTU, respectively, which decreased by 22.0, 13.0, 29.8, and 21.3%, respectively, compared to the initial turbidity (Fig. 7(a)). The corresponding effluent turbidity of permeate was finally stable at 0.05 NTU, 0.06 NTU, 0.08 NTU, and 0.08 NTU, respectively, all below 0.1 NTU. It indicated that very small amount of MgO(111) nanosheets permeated and the decreased MgO(111) in the solution primarily adsorbed on the membrane. The result was further confirmed by the mass balance of MgO(111). The concentration of MgO(111) inside the reactor was tracked. It decreased at first and then reached a steady-state value of 0.48, 0.93, 1.42, and 1.83 g/L, respectively (Fig. 7(b)). The adsorbed MgO(111) on

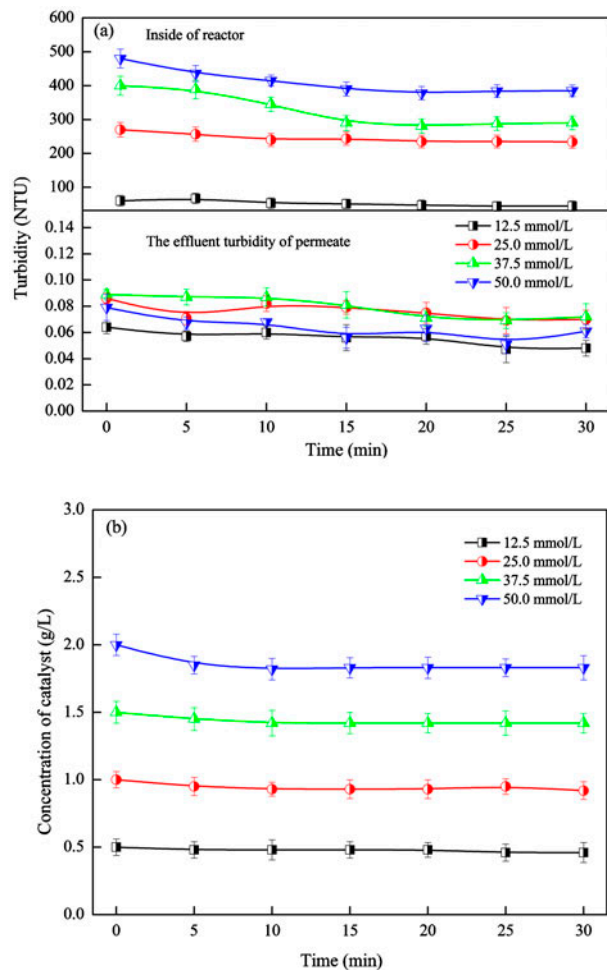


Fig. 7. (a) Turbidity changes at different MgO(111) dosages; (b) Concentrations of MgO(111) inside the reactor at different initial dosages (TMP: 8.0 kPa; NB: 50.0 mg/L; pH: 6.7).

the surface of the membrane and the permeated MgO(111) particles could explain the initial decrease in the turbidity of the mixed liquor and the concentration of MgO(111) inside the reactor. After reaching the steady state in 20 min, the adsorption and desorption equilibrium of MgO(111) particles on the surface of the immersed membrane was established. Since the quantity of MgO(111) in the effluent is very small indicated by the turbidity, lower than 0.1 NTU, the effluent sample in each case at 20 min was digested and the concentration of magnesium ion was measured by ICP, which was 1.2, 1.8, 1.9, and 1.8 mg/L corresponding to the MgO(111) dosage of 12.5, 25.0, 37.5 and 50.0 mmol/L. Thus, the permeated MgO(111) was estimated as 2.0, 3.0, 3.2, and 3.0 mg/L. According to the mass balance, the adsorbed MgO(111) on the surface of the membrane was 18.0, 67.0, 76.8, and 167.0 mg/L, respectively. After reaching the steady

state in 20 min, the dynamic membrane with the adsorbed MgO(111) cake formed and played a better role of intercepting the catalyst particles than the raw membrane. The measurements of both turbidity and catalyst concentration showed that the ceramic membrane could almost intercept the MgO(111) particles inside the reactor during operation, which hence could be reused in a continuous flow mode without additional recovery from the treated water. The successful retention of MgO(111) particles by the membrane in HCOM reactor also indicates that the commercial ceramic membrane with an average surface pore size of  $3.0\ \mu\text{m}$  is suitable. The HCOM reactor overcomes the shortcomings of the usual way (coagulation, gravity settling, and filtration) to reuse the catalyst, such as complication, discontinue, and time wasting. For example, coagulation and flocculation, as conventional methods to remove catalyst from the treated water, would use flocculants to enhance sedimentation, so that an additional separation process is required. The novel HCOM reactor could continuously treat wastewater, which would avoid the additional separation of catalyst for reuse and save much time. Thus, the treatment capacity of the reactor and the treatment efficiency of aqueous organic pollutants were enhanced greatly.

### 3.3.2. Membrane fouling in HCOM reactor

The decrease in permeate flux can indicate the membrane fouling in HCOM reactor. Hence, the permeate fluxes of the membrane separation process with different MgO(111) concentrations were measured, as shown in Fig. 8. The permeate fluxes were kept almost constant at the MgO(111) concentration of 12.5 and 25.0 mmol/L, but when the MgO(111) concentration of 37.5 and 50.0 mmol/L used, the permeate fluxes decreased. It is important to note that the fluxes declined obviously during initial filtration, and then slowly, finally reached a relatively steady state after about 20 min operation. The residual MgO(111) concentration inside the reactor also changed in the same trend. Moreover, the permeate fluxes decreased more quickly when higher concentration of MgO(111) was used, indicating that the membrane fouling increased exponentially with an increase of MgO(111) concentration. According to the above discussion, most of the decreased MgO(111) was adsorbed by the membrane and the adsorbed amount also increased by increasing the MgO(111) concentration. The adsorbed particles formed a cake lake on the surface of the membrane or even penetrated the membrane to block the pores, which resulted in the membrane fouling [42].

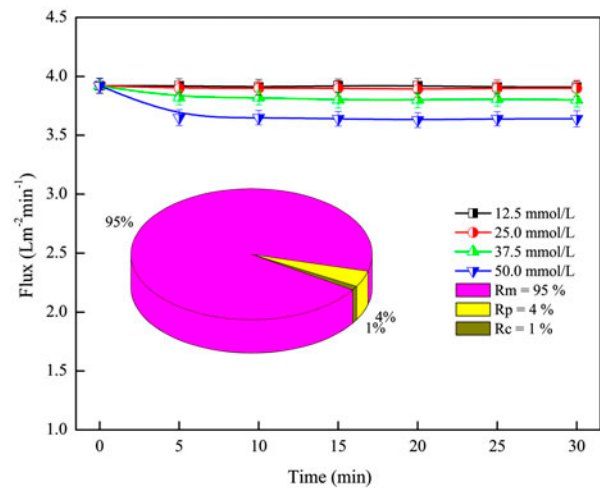


Fig. 8. Membrane flux changes in the continuous reactor with different MgO(111) concentrations and resistance constitution of the used membrane (TMP: 8.0 kPa; NB: 50.0 mg/L; pH: 6.7).

Therefore, the membrane fluxes declined and the membrane resistance increased when the catalyst concentration increased. To examine the fouling mechanism, component membrane resistances after 30 min operation of the HCOM reactor with 25.0 mmol/L MgO(111) catalyst was measured (the inset of Fig. 8). The total resistance ( $R_t$ ) was  $123.07 \times 10^9\ \text{m}^{-1}$ , including cake resistance ( $R_c$ ), pore plugging resistance ( $R_p$ ), and intrinsic membrane resistance ( $R_m$ ) of  $1.23 \times 10^9\ \text{m}^{-1}$ ,  $4.92 \times 10^9\ \text{m}^{-1}$ , and  $116.92 \times 10^9\ \text{m}^{-1}$ , respectively. The membrane fouling was mainly resulted by the MgO(111) deposited on the membrane and in the pores of the membrane. The fouling degree can be indicated by the cake resistance and pore plugging resistance. These two resistances occupying only 5.0% of the total resistance showed that only slight membrane fouling occurred.

### 3.3.3. Long-term catalytic degradation of NB in HCOM reactor

Long-term catalytic degradation of NB in HCOM reactor was carried out to evaluate the stability of the integrated HCOM separation system, and reuse of the catalyst. The HCOM reactor was operated based on the above determined operation parameters, such as catalyst type and dosage, the initial solution pH, the membrane type, and the permeate flux. As shown in Fig. 9, the NB removal rate increased rapidly, and reached about 90% at 30 min, and then kept constant even during the 24 h operation. It implied that MgO

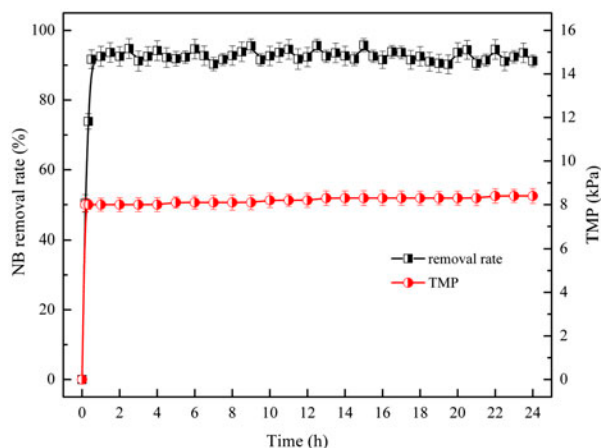


Fig. 9. Removal rate of NB and TMP changes in the HCOM reactor (MgO: 25.0 mmol/L; O<sub>3</sub>: 5.0 mg/L; NB: 50.0 mg/L; pH: 6.7).

(111) nanosheets were durable without significant loss in catalytic activity. At the same time, the TMP was almost kept constant at about 8.0 kPa and only slightly increased with the time, indicating that the membrane fouling was minor even after 24 h operation. The treatment capacity of the continuous flow HCOM reactor reached 48.0 L/d while that of the batch reactor with the same working volume should be much lower due to the time-wasting recovery of catalyst between two runs and the loss of the catalyst during the recovery operation.

The integrated HCOM separation system was very steady in the long-term operation and the catalyst particles could be mostly rejected. The long-term experiment indicated that the HCOM system was efficient for degradation of refractory organic pollutants in water. Even if deactivation of the catalyst occurred in the integrated system, fresh catalyst can be introduced simply.

#### 4. Conclusions

The integrated HCOM separation system with active MgO catalyst is proved to be feasible for efficient removal of refractory organic pollutants in water and retention of fine size catalyst conveniently. MgO nanosheets with dominant (111) facets were prepared successfully by facile wet chemical process, which exhibited higher catalytic activity than both CP-MgO and the most extensively studied MnO<sub>x</sub> due to a high concentration of surface O<sup>2-</sup> Lewis basic sites on the unusual surface. In addition, the HCOM system can realize continuous reuse of MgO(111) catalysts. Thus, the treatment capacity of the reactor and the treatment

efficiency of refractory organic pollutants were enhanced greatly. The measurements of the turbidity and the residual concentration of MgO(111) suspended in the reactor showed that the catalysts were successfully retained in the reactor by the membrane. At the optimum 25.0 mmol/L dosage of MgO(111), 5% contribution of the total resistance brought by cake and pore plugging resistance indicated that the membrane fouling was negligible. The long-term continuous catalytic ozonation experiments demonstrated that the removal rate of NB could maintain over 90% with a constant flux of 3.92 L m<sup>-2</sup> min<sup>-1</sup> during the 24 h operation. These results showed that this integrated heterogeneous catalytic ozonation based on active MgO(111) catalyst and membrane separation was confirmed to be efficient for degradation of recalcitrant organic pollutants in wastewater.

#### Acknowledgments

This research was supported by Nature Science Foundations of China (20977117, 21107146), Nature Foundations of Guangdong Province (9251002750 1000005), Science and Technology Research Programs of Guangzhou City (2012J4300118) and Project of Education Bureau of Guangdong Province (cghzd1001), the Fundamental Research Funds for the Central Universities (121pgy20), and the Academic scholarship for new person of education ministry in China.

#### References

- [1] B. Legube, N.K.V. Leitner, Catalytic ozonation: A promising advanced oxidation technology for water treatment, *Catal. Today* 53 (1999) 61–72.
- [2] R. Andreozzi, V. Caprio, A. Insola, R. Marotta, Advanced oxidation processes (AOP) for water purification and recovery, *Catal. Today* 53 (1999) 51–59.
- [3] M.A. Alsheyab, A.H. Muñoz, Comparative study of ozone and MnO<sub>2</sub>/O<sub>3</sub> effects on the elimination of TOC and COD of raw water at the Valmayor station, *Desalination* 207 (2007) 179–183.
- [4] M. Mehrjouei, S. Müller, D. Möller, Synergistic effect of the combination of immobilized TiO<sub>2</sub>, UVA and ozone on the decomposition of dichloroacetic acid, *J. Environ. Sci. Health Part A* 47 (2012) 1073–1081.
- [5] R.C. Martins, R.M. Quinta-Ferreira, Manganese-based catalysts for the catalytic remediation of phenolic acids by ozone, *Ozone Sci. Eng.* 31 (2009) 402–411.
- [6] Y.L. Nie, C. Hu, N.N. Li, L. Yang, J.H. Qu, Inhibition of bromate formation by surface reduction in catalytic ozonation of organic pollutants over beta-FeOOH/Al<sub>2</sub>O<sub>3</sub>, *Appl. Catal. B-Environ.* 147 (2014) 287–292.
- [7] M. Leili, G. Moussavi, K. Naddafi, Degradation and mineralization of furfural in aqueous solutions using heterogeneous catalytic ozonation, *Desalin. Water Treat.* 51 (2013) 6789–6797.

- [8] Y. Dong, H. Yang, K. He, X. Wu, A. Zhang, Catalytic activity and stability of Y zeolite for phenol degradation in the presence of ozone, *Appl. Catal. B-Environ.* 82 (2008) 163–168.
- [9] K. Zhu, J. Hu, C. Kübel, R. Richards, Efficient preparation and catalytic activity of MgO(111) nanosheets, *Angew. Chem. Int. Ed.* 118 (2006) 7435–7439.
- [10] N. Engelhardt, W. Firk, W. Warnken, Integration of membrane filtration into the activated sludge process in municipal wastewater treatment, *Water Sci. Technol.* 38 (1998) 429–436.
- [11] H. Liu, C. Yang, W. Pu, J. Zhang, Removal of nitrogen from wastewater for reusing to boiler feed-water by an anaerobic/aerobic/membrane bioreactor, *Chem. Eng. J.* 140 (2008) 122–129.
- [12] T. Liu, Z.L. Chen, W.Z. Yu, S.J. You, Characterization of organic membrane foulants in a submerged membrane bioreactor with pre-ozonation using three-dimensional excitation-emission matrix fluorescence spectroscopy, *Water Res.* 45 (2011) 2111–2121.
- [13] J. Wu, X. Huang, Use of ozonation to mitigate fouling in a long-term membrane bioreactor, *Bioresour. Technol.* 101 (2010) 6019–6027.
- [14] L.M. Corneal, M.J. Baumann, S.J. Masten, S.H. Davies, V.V. Tarabara, S. Byun, Mn oxide coated catalytic membranes for hybrid ozonation-membrane filtration: Membrane microstructural characterization, *J. Membr. Sci.* 369 (2011) 182–187.
- [15] S. Byun, S. Davies, A. Alpatova, L. Corneal, M. Baumann, V. Tarabara, S. Masten, Mn oxide coated catalytic membranes for a hybrid ozonation-membrane filtration: Comparison of Ti, Fe and Mn oxide coated membranes for water quality, *Water Res.* 45 (2011) 163–170.
- [16] B. Karnik, M. Baumann, S. Masten, S. Davies, AFM and SEM characterization of iron oxide coated ceramic membranes, *J. Mater. Sci.* 41 (2006) 6861–6870.
- [17] J. Kim, W. Shan, S.H. Davies, M.J. Baumann, S.J. Masten, V.V. Tarabara, Interactions of aqueous NOM with nanoscale TiO<sub>2</sub>: Implications for ceramic membrane filtration-ozonation hybrid process, *Environ. Sci. Technol.* 43 (2009) 5488–5494.
- [18] S. Bamperng, T. Suwannachart, S. Atchariyawut, R. Jiratananon, Ozonation of dye wastewater by membrane contactor using PVDF and PTFE membranes, *Sep. Purif. Technol.* 72 (2010) 186–193.
- [19] K.C. Chen, S.H. Davies, S.J. Masten, Mass transfer of ozone in a hybrid ozonation-membrane system, *J. Adv. Oxid. Technol.* 10 (2007) 287–296.
- [20] S. Contreras, M. Rodríguez, E. Chamarro, S. Esplugas, UV- and UV/Fe(III)-enhanced ozonation of nitrobenzene in aqueous solution, *J. Photochem. Photobiol., A* 142 (2001) 79–83.
- [21] J. Hu, K. Zhu, L. Chen, C. Kübel, R. Richards, MgO (111) nanosheets with unusual surface activity, *J. Phys. Chem. C* 111 (2007) 12038–12044.
- [22] X. Zhang, J.H. Pan, A.J. Du, W. Fu, D.D. Sun, J.O. Leckie, Combination of one-dimensional TiO<sub>2</sub> nanowire photocatalytic oxidation with microfiltration for water treatment, *Water Res.* 43 (2009) 1179–1186.
- [23] M. Verziu, B. Cojocaru, J. Hu, R. Richards, C. Ciuculescu, P. Filip, V.I. Parvulescu, Sunflower and rapeseed oil transesterification to biodiesel over different nanocrystalline MgO catalysts, *Green Chem.* 10 (2008) 373–381.
- [24] J. Nawrocki, B. Kasprzyk-Hordern, The efficiency and mechanisms of catalytic ozonation, *Appl. Catal. B-Environ.* 99 (2010) 27–42.
- [25] Z. Liu, J.A. Cortés-Concepción, M. Mustian, M.D. Amiridis, Effect of basic properties of MgO on the heterogeneous synthesis of flavanone, *Appl. Catal. A-Gen.* 302 (2006) 232–236.
- [26] G. Moussavi, A.A. Aghapour, K. Yaghmaeian, The degradation and mineralization of catechol using ozonation catalyzed with MgO/GAC composite in a fluidized bed reactor, *Chem. Eng. J.* 249 (2014) 302–310.
- [27] K. Tomita, Y. Oshima, Enhancement of the catalytic activity by an ion product of sub- and supercritical water in the catalytic hydration of propylene with metal oxide, *Ind. Eng. Chem. Res.* 43 (2004) 2345–2348.
- [28] N. Sahai, Is silica really an anomalous oxide? Surface acidity and aqueous hydrolysis revisited, *Environ. Sci. Technol.* 36 (2002) 445–452.
- [29] R. Huang, H. Yan, L. Li, D. Deng, Y. Shu, Q. Zhang, Catalytic activity of Fe/SBA-15 for ozonation of dimethyl phthalate in aqueous solution, *Appl. Catal. B-Environ.* 106 (2011) 264–271.
- [30] L. Zhao, J. Ma, Z.Z. Sun, X.D. Zhai, Catalytic ozonation for the degradation of nitrobenzene in aqueous solution by ceramic honeycomb-supported manganese, *Appl. Catal. B-Environ.* 83 (2008) 256–264.
- [31] S.P. Tong, R. Shi, H. Zhang, C.A. Ma, Kinetics of Fe<sub>3</sub>O<sub>4</sub>-CoO/Al<sub>2</sub>O<sub>3</sub> catalytic ozonation of the herbicide 2-(2, 4-dichlorophenoxy) propionic acid, *J. Hazard. Mater.* 185 (2011) 162–167.
- [32] B. Kasprzyk-Hordern, M. Ziółek, J. Nawrocki, Catalytic ozonation and methods of enhancing molecular ozone reactions in water treatment, *Appl. Catal. B-Environ.* 46 (2003) 639–669.
- [33] L. Lei, L. Gu, X. Zhang, Y. Su, Catalytic oxidation of highly concentrated real industrial wastewater by integrated ozone and activated carbon, *Appl. Catal. A-Gen.* 327 (2007) 287–294.
- [34] L. Zhao, J. Ma, Z. Sun, X. Zhai, Mechanism of influence of initial pH on the degradation of nitrobenzene in aqueous solution by ceramic honeycomb catalytic ozonation, *Environ. Sci. Technol.* 42 (2008) 4002–4007.
- [35] T. Zhang, C. Li, J. Ma, H. Tian, Z. Qiang, Surface hydroxyl groups of synthetic  $\alpha$ -FeOOH in promoting OH generation from aqueous ozone: Property and activity relationship, *Appl. Catal. B-Environ.* 82 (2008) 131–137.
- [36] T.F. de Oliveira, O. Chedeville, B. Cagnon, H. Fauduet, Degradation kinetics of DEP in water by ozone/activated carbon process: Influence of pH, *Desalination* 269 (2011) 271–275.
- [37] L. Huang, D.Q. Li, Y.J. Lin, M. Wei, D.G. Evans, X. Duan, Controllable preparation of nano-MgO and investigation of its bactericidal properties, *J. Inorg. Biochem.* 99 (2005) 986–993.
- [38] C. Hu, S. Xing, J. Qu, H. He, Catalytic ozonation of herbicide 2,4-D over cobalt oxide supported on mesoporous zirconia, *J. Phys. Chem. C* 112 (2008) 5978–5983.
- [39] Y. Ren, Q. Dong, J. Feng, J. Ma, Q. Wen, M. Zhang, Magnetic porous ferrosipinel NiFe<sub>2</sub>O<sub>4</sub>: A novel ozonation catalyst with strong catalytic property for

- degradation of di-n-butyl phthalate and convenient separation from water, *J. Colloid Interface Sci.* 382 (2012) 90–96.
- [40] F. Qi, B. Xu, Z. Chen, L. Feng, L. Zhang, D. Sun, Catalytic ozonation of 2-isopropyl-3-methoxypyrazine in water by  $\gamma$ -AlOOH and  $\gamma$ -Al<sub>2</sub>O<sub>3</sub>: Comparison of removal efficiency and mechanism, *Chem. Eng. J.* 219 (2013) 527–536.
- [41] A. Cherkasov, A. Polotsky, Critical particle-to-pore size ratio in ultrafiltration, *J. Membr. Sci.* 106 (1995) 161–166.
- [42] L.D. Nghiem, S. Hawkes, Effects of membrane fouling on the nanofiltration of pharmaceutically active compounds (PhACs): Mechanisms and role of membrane pore size, *Sep. Purif. Technol.* 57 (2007) 176–184.